MODELLING AND SIMULATION OF THE PROPAGATION CHARACTERISTICS OF THE 900 MHz NARROWBAND-TDMA CEPT/GSM MOBILE RADIO (*)

G.D'ARIA, L.STOLA, and V.ZINGARELLI

CSELT - Centro Studi e Laboratori Telecomunicazioni
Via Reiss Romoli 274 - I 10148 Torino (Italy)

Abstract

This paper is concerned with the problem of modelling and simulating the propagation characteristics for the new pan-European 900 MHz digital mobile radio system, as specified by CEPT/GSM. Together with COST Project 207, CEPT/GSM has also defined propagation models for a few "typical terrains", i.e., the rural, urban, bad-case urban, and hilly terrains.

The modelling problem is solved by means of a Time and Frequency-dependent Linear Filter (TFLF) identified by its transfer function and representative of the short-term random propagation processes. Starting from such a TFLF and from the "power delay profiles" specified by CEPT/GSM, the simulation model provides independent realizations of the mobile radio channel transfer function. Particular attention is also devoted to the model calibration.

Finally, an example of performance analysis is shown, considering a typical communication channel of the CEPT/GSM system employing a reduced-complexity Viterbi adaptive equalizer, based on a modified Viterbi algorithm, and with timing and carrier phase recovery and channel impulse response estimation performed by exploiting the 26-bit "midamble" sequence foreseen by the TDMA channel burst format.

I. INTRODUCTION

The CEPT/GSM pan-European digital mobile radio system to be put into service at the end of 1991 [1], [2] envisages a Time Division Multiple Access (TDMA), with 8 channels per carrier.

In such a mobile system the signal received by the moving vehicle is usually strongly affected by the surrounding environment: natural and man made obstacles, hills and buildings seldom allow a line of sight path between transmitter and receiver to be established. As a consequence, at the mobile station the signal usually consists of multipath components due to diffusion, diffraction and scattering. The simple random relative position of the mobile unit with respect to obstacles does not provide a satisfactory deterministic propagation model and forces a statistical approach to the channel characterization.

The first part of this paper is devoted to examine the "short-term" (or "fast") random process characterizing the mobile radio channel, including its frequency selective properties. Frequency selectivity effects, caused by the different delays of the multipath components, are of paramount importance when the transmission rate is greater than the "coherence bandwidth", since they lead to intersymbol interference and increase the bit error ratio of the data transmission. To define the propagation model, it is assumed that the communication channel between base and mobile stations can be formally handled as a Time and Frequency-dependent Linear Filter (TFLF) model, identified by its transfer function H(t,f) representative of the above mentioned short-term random process.

The second part of the paper is devoted to the software simulation of the fast mobile radio propagation channel according to the different models defined by CEPT/GSM [3]. Starting from the TFLF model, we suggest a computer technique to simulate samples of the transfer function in the time-frequency domain. The dynamic channel is simulated by means of indipendent samples of H(t,f), generated as a realization of the short-term random process, in a given environment. We pay particular attention to the model calibration, by investigating the relationship between the mobile channel transfer function and the most important parameters that depend on the environmental characteristics: the distribution (usually referred to as "power delay profile") of multipath time delays [4] and, for a given vehicle speed, the Doppler spectrum (which can be modelled both in shape and width). Even if our attention is limited to the urban and suburban areas, identified by means of the particular power delay profile defined by CEPT/GSM, different environments can be described by ad hoc selections of the corresponding random process parameters.

Moreover, we make use of the simulation procedure to investigate some transfer function properties on which few experimental results are avaliable. For example, the autocorrelation function [20], both in the frequency (coherence bandwidth) and time domains.

The third part of the paper deals with the performance analysis of the CEPT/GSM system over the abovementioned propagation channels, considering the necessary countermeasure technique for the frequency selective distortions, i.e., adaptive baseband equalization. The simulations have been carried out by a software package named TDMAGSM, developed at CSELT in the framework of the studies on the GSM system [8,10, 11,26]. Two main classes of adaptive receivers [6] have been considered in previous works: 1) linear tranversal equalizers and nonlinear decision-feedback equalizers [7-11]; 2) receivers employing maximum-likelyhood sequence estimation (e.g., the Viterbi algorithm, [10-11]) made adaptive at least during a preamble period by means of some sort of channel estimation. By using the new modelling and simulation technique herewith presented, this paper gives results on the performance of adaptive equalizers using the Viterbi algorithm, designed to meet the CEPT/GSM requirements.

II. PROPAGATION CHANNEL MODELLING (TFLF MODEL)

As said in Section I, at the mobile station the signal usually consists of multipath components, arising from diffusion, diffraction and scattering due to surrounding obstacles. Each multipath component can be thought as an independent travelling plane wave, whose amplitude, phase, incoming angle and time delay are random variables. As a consequence, the mobile propagation channel is described by a random process,

(*) This work has been sponsored by SIP, the Italian Telephone Operating Company

CH2379-1/89/0000/0631 $1.00 © 1989 IEEE

whose statistical characteristics are to be investigated [12-15]. To state the stationarity in the time (or space) domain of such a random process it can be useful to suppose the mobile channel as the result of two overlapping processes, both stationary, characterized by different periodicities. The "slow" random process, usually known as "shadowing", is related to the large scale fluctuations; for example, in an urban area, it is related to the density and to the average height of the buildings or to the width of the streets. This process is assumed to be stationary over some hundreds of metres and the received signal is log-normally distributed [16], [17]. The short-term random process is mainly related to the motion of the mobile station through the spatial standing wave pattern [18] resulting from the local multipath interference and is responsible for the fluctuations of the propagation channel within fractions of a wavelength. This process can be supposed stationary over some tens of wavelengths (on the order of 4-5 metres, in the 900 MHz band) and with statistics of the Rayleigh type. The short term mobile radio channel in both built-up and open areas is conveniently characterized by its transfer function H(t,f), supposed to be time-frequency factorized. Such a factorization hypothesis does not restrict the model reliability and flexibility and plays a fundamental role in the calibration and simulation procedures. In what follows only the real part of H(t,f) will be dealt with, since similar considerations hold for the imaginary part.

Let us consider the time evolution of $Re\{H(t,f_c)\}$ at a fixed frequency (i.e., the carrier frequency f_c). According to the usual formalism related to the discrete Fourier series expansion, we have

$$Re\{H(t,f_c)\}=A_0(f_c)+2\{\sum_{n=1}^{N-1}[A_n(f_c)\cos(n\nu_0 t)+ B_n(f_c)\sin(n\nu_0 t)]\}+A_N(f_c)\cos(N\nu_0 t) \quad (1)$$

where N is the number of harmonics required in order to give a satisfactory description of the time evolution, ν_0 is the fundamental harmonic of the series expansion and $\{A_n(f_c),B_n(f_c)\}$ is a set of frequency-dependent and time-constant coefficients. The parameter $T=1/\nu_0$ is the time duration of the sample of $H(t,f_c)$ and it must fall in the stationarity range of the corresponding random process. If all modulation phenomena occur in the frequency domain f, then the frequency domain ν is the narrow band (wide a few hundreds of kHz) centered around the carrier frequency, containing all the spurious modulation products induced by the vehicle motion (i.e., the "random Frequency Modulation", FM).

The bandwidth $N\nu_0$ in (1) is the well known Doppler bandwidth and depends on the environment and the vehicle speed. As this spurious random FM bandwidth increases, the received noise floor increases. The coefficient set $\{A_n(f_c),B_n(f_c)\}$ determines the shape of the Doppler spectrum at a given f_c and depends on the distribution of the angles of incidence of the incoming multipath components at the mobile station [13], [14]. The fine characterization of the channel transfer function within a given frequency band requires the knowledge of a sufficient number of sets $\{A_n(f),B_n(f)\}$. The number ensuring a satisfactory discrete description of the propagation model depends on the transmitted signal bandwidth and on the dynamic properties of the transfer function, i.e., on the rapidity of the transfer function fluctuations vs frequency.

In order to properly describe the frequency characteristics of the mobile propagation channel in the modulation bandwidth, a new formal approach, with an equivalent information content, can be adopted. To this purpose, the discrete Fourier series expansion of the real part of the instanteneous (i.e., at $t=t_0$) transfer function can be written as

$$Re\{H(t_0,f)\} = \mathcal{A}_0(t_0)+2\{\sum_{m=1}^{M-1}[\mathcal{A}_m(t_0)\cos(m\tau_0 f)+ \mathcal{B}_m(t_0)\sin(m\tau_0 f)]\}+\mathcal{A}_M(t_0)\cos(M\tau_0 f) \quad (2)$$

In this case τ runs in the echo time delay domain.

As known, the time delay spectrum determines the frequency selectivity of the channel and plays a role similar to that of the Doppler spectrum in determining the time selectivity. According to such an interpretation, in (2) $F=1/\tau_0$ is the bandwidth where the description of the frequency selectivity effects is restricted, whereas $M\tau_0$ is the maximum delay corresponding to the environment under examination. The higher $M\tau_0$ is, the faster the transfer function fluctuations vs frequency are.

The coefficient set $\{\mathcal{A}_m(t_0),\mathcal{B}_m(t_0)\}$ determines the shape of the instantaneous delay spectrum.

As before, in order to know the time evolution characterization of the transfer function with a proper time resolution, the knowledge of a sufficient number of sets is required. As regards the coefficient sets in (1) and (2), to make the model handling easier without loss of accuracy, the following two hypotheses can be done:

$$[A_n^2(f)+B_n^2(f)]_{f\epsilon f_s} = |S_n|^2 \quad (3a)$$

$$[\mathcal{A}_m^2(t)+\mathcal{B}_m^2(t)]_{t\epsilon t_s} = |T_m|^2 \quad (3b)$$

Hypothesis (3a) implies that the Doppler spectrum is frequency-independent in the stationarity band f_s, i.e., both statistical and dynamic properties of the time evolution of H(t,f) are frequency independent, for a given environment and a given mobile speed. For example, with f_c=900 MHz, if variations of the Doppler spectrum up to 1% are accepted, the stationarity band is about 10 MHz because the Doppler spectrum bandwidth is linearly proportional to the carrier frequency (for fixed speed and angle of incidence).

Hypothesis (3b) implies that the time-delay spectrum is time-independent during the stationarity period t_s, i.e., the in-band selectivity characteristics are constant.

The time period during which an urban channel can be represented as a stationary process is about 1s at 50 km/h, if the transmitted signal bandwidth is supposed to be narrow (20-30 kHz). Hypothesis (3a) is more stringent, because it has to be verified within wider bandwidths (a few hundreds of kHz for the CEPT/GSM system). For such systems, measurements of the time evolution of delay profile in various environments [4] suggest tentative average values of t_s on the order of tens of ms (or less).

All the simulation results presented in the following section are based on hypotheses (3a) and (3b).

The TFLF model outlined above shows its advantages in the H(t,f) simulation and calibration procedures, which have to take account of the physical values obtained by measurements. In fact, as shown in what follows, generally, such values are closely related to the spectral behavior in the frequency bandwidth ν around f_c ($\{A_n(f),B_n(f)\}$ set) and in the time delay domain τ ($\{\mathcal{A}_m(t),\mathcal{B}_m(t)\}$ set).

III. SOFTWARE SIMULATION

The study of time evolution, for a fixed frequency f_c, of a mobile channel requires the knowledge of the Doppler power spectral density of the real and imaginary parts of $H(t,f_c)$. Since the model software simulation requires a discrete formalism, the following approach is similar to that proposed by Aulin [5] for his non-plane propagation model. To this purpose, a

parabolic shape of $|S_n|^2$ is assumed to represent the Doppler frequency band ($|S_n|^2=0$ out of this band); such a shape seems to be particularly suited to numerical computations.

The simulation process basically consists of two parallel and independent computational flows, one for $Re\{H(t,f_c)\}$ and the other for $Im\{H(t,f_c)\}$. Starting from the shape $|S_n|^2$, and simulating spectral amplitudes with uniformly distributed phases, the complex quantity S_n is evaluated (coefficient set $\{A_n(f_c),B_n(f_c)\}$). Assuming the real and imaginary part to be even and odd, respectively, the complex quantity S_n can be interpreted as the Fourier transform of a real signal. Two independent inverse Fourier transforms, numerically performed by a FFT technique, give the time realization of the real and imaginary parts of the channel transfer function relative to an urban multipath environment. A different environment, such as a suburban or rural area, can be simulated by adding a deterministic component to the trasfer function simulated as described above. Such a deterministic component stands for the main and constant propagation path, characterized by a power ρ, relative to that of the random multipath component.

The value of the angle α_m between the main-component arrival direction and the vehicle direction is irrelevant to the overall transfer function statistical time evolution. α_m=45° is assumed as well representative of a typical average environment.

The power ratio ρ appears to be an important parameter. For low values of ρ (~0 dB) random contributions prevail, which reflect into a Rayleigh distribution for $|H(t,f_c)|$; it can be shown that even a moderate increase of ρ (from 5 to 10 dB) causes remarkable changes in both statistical and dynamic properties of the transfer function.

Investigations about the possible relationship between ρ and the urban structure are beyond the scope of this work; nevertheless, on the basis of a qualitative interpretation of some experimental results [15], [17], the following classification is drawn:

a) Urban centre - high building density (>30%): ρ=-∞dB (only multipath component)
b) Urban area - moderate building density (20%÷30%): ρ=0÷4dB
c) Urban area - low building density (10%÷20%): ρ=4÷6dB
d) Suburban area: ρ=6÷10dB
e) Open (or rural) area: ρ>10dB.

In any case, for a fixed environment, by using the simulation technique described above and a HP 9020 desk-top computer, a CPU time of about 1 minute provides a realization of $H(t,f_c)$ with a time duration of 0.8 s (f_c=900 MHz, mobile speed v=50 km/h, time resolution $5\cdot10^{-5}$ s). The statistical stability of the simulated quantities is achieved after some hundreds of realizations, therefore 3 to 4 CPU-hours are required.

Some simulation results are reported for 5 different propagation channels, characterized by ρ equal to -∞, 2, 5, 8, 12dB. Notice that the adopted mobile speed (50 km/h) is implicitely considered because the results are presented in terms of travelled distances. Also the carrier frequency is kept costant.

In Fig. 1 the spectral power densities of $Re\{H(t,f_c)\}$ (or $Im\{H(t,f_c)\}$), obtained by averaging 300 simulated realizations (for each value of ρ), are reported. In the curve (a) (ρ=-∞) only the random multipath channel is present, whereas the other curves experience the effects of the increasing of the deterministic component.

As regards $|H(t,f_c)|$, the simulated statistics for ρ=-∞ are not distinguishable from the theoretical Rayleigh distribution; as the deterministic component increases, the envelope statistics approach the Rice distribution [19]. Fig. 2 shows the average level crossing rate of $|H(t,f_c)|$, normalized to the Doppler bandwidth, as usually done in the literature. According to such a normalization, the resulting behavior is independent of mobile speed and carrier frequency. It is worth noting that ρ affects to a large extent also the dynamic properties of $|H(t,f_c)|$. On the other hand, it has no practical influence on the statistical properties of the phase $\phi_H(t,f_c)$ of the transfer function. In fact, in this case the distribution is uniform in $[-\pi,\pi]$, irrespective of the value of ρ.

A more exaustive investigation on the channel time variations can be obtained by computing the derivatives vs space of $|H(vt,f_c)|$ and $\phi_H(vt,f_c)$. Fig. 3 reports the distribution of the space-derivative of $|H(vt,f_c)|$ (dB/cm) for the five above-quoted environments. Fig. 4 is relevant to the cuncurrent space-derivatives of $\phi_H(vt,f_c)$ (deg/cm).

Such a channel evolution can be also examined by means of the $|H(vt,f_c)|$ autocorrelation characteristics: Fig. 5 depicts the space autocorrelation function for ρ equal to -∞ and 5 dB. It is worth noting that the presence of a deterministic component increases the values of the autocorrelation.

As far as the frequency selective characteristics are concerned, we start from the delay profile of the incoming echoes, i.e., the impulse response of the TFLF, representative of the short-term propagation characteristics. The longer the impulse response is, the heavier the effects due to in-band distortion phenomena are, just as a wider Doppler spectrum results into higher time dynamics. Consequently, a suitable model to simulate instantaneous realizations of the transfer function $H(t_0,f)$ can be obtained from the previous model by simply exchanging time with frequency. However, an important difference, at least in principle, has to be highlighted: in the simulation of $H(t_0,f)$, all echoes, whatever their delay or associated power, are handled as potential sources of in-band distortions and no echo can be identified as a main (or deterministic) signal. Also in this case, two independent and parallel branches are simulated in order to compute $Re\{H(t_0,f)\}$ and $Im\{H(t_0,f)\}$ starting from their delay spectra, respectively.

The first simulation step deals with the power spectral density $|T_m|^2$ of delays; a generic simulation of phases, assumed uniformely distributed in the range $[-\pi,\pi]$, leads to the complex form of T_m (i.e., the coefficient set $\{\mathcal{A}_m(t_0),\mathcal{B}_m(t_0)\}$). Introducing the usual simmetry assumption, the Fourier transform of a real signal is obtained. The inverse Fourier transform (FFT) gives $Re\{H(t_0,f)\}$ as a function of frequency. Similarly, the other simulation branch furnishes $Im\{H(t_0,f)\}$.

The so obtained transfer function $H(t_0,f)$ is a single realization of the random process characterized by the delay spectrum $|T_m|^2$, and depends on the considered environment and on f_c.

Finally, a satisfactory relationship between the environment and $|T_m|^2$ remains to be faced. Unfortunately, most available experimental results have been obtained using an impulse technique and provide only the amplitude delay profiles (i.e., the delay profiles of $|H(t_0,f)|$): no information about the phase (or about both the real and the imaginary parts of the transfer function) is usually available.

Therefore, one needs a proper analytical method to calibrate the model on the basis of the experimental data and, consequently, to obtain the spectrum of both the real and imaginary parts starting from the experimental amplitude.

An alternative method, herewith used, is based on an iterative procedure that provides, by successive approximations, the spectral profiles $|T_m|^2$ of $Re\{H(t_0,f)\}$ and $Im\{H(t_0,f)\}$ (corresponding to measured or proposed delay profiles of $|H(t_0,f)|$) to be used as inputs to the simulation process.

An example of model calibration, obtained by using the above mentioned iterative method, is reported in Fig. 6. Dashed line (a) is the CEPT/GSM [3] time delay

profile of $|H(t_0,f)|$ for a 900 MHz urban and suburban mobile channel. Curve (b) represents the spectral profile $|T_m|^2$ of $Re\{H(t_0,f)\}$ (or $Im\{H(t_0,f)\}$) and is characterized by an exponentially decreasing behavior (mean value and standard deviation equal to 0.65 μs). By starting from $|T_m|^2$, our simulation model provides instantaneous samples of $H(t_0,f)$ in a bandwidth of about 8 MHz centered around f_c with a frequency step of 1 kHz. The mean spectral delay profile of $|H(t_0,f)|$ is then computed by averaging 300 independently simulated profiles. The result is reported as curve (c) in Fig. 6. It is worth noting that curve (c) fits (a) well. Then the delay profile (c) used in our simulation model can stand for the urban and suburban propagation channel proposed by CEPT/GSM (notice that the portion of spectrum beyond 7 μs is practically negligible, because of its poor power content).

The simulation process is able to give some statistical information on the frequency selectivity of the simulated propagation channel, as well. For example, the instantaneous modulus of the transfer function is still Rayleigh distributed, as shown in Fig.7. It also shows the mean level crossing rate on a 270 kHz bandwidth (according to the CEPT/GSM signal bandwidth). Fig. 8 reports the statistics of the derivatives of modulus (dB/kHz) and phase (deg/kHz), from which informations about the rate of variations can be easily drawn. Fig. 9 shows the $|H(t_0,f)|$ autocorrelation vs frequency on a bandwidth of 270 kHz. Notice that the results of Fig. 9 agree with the measurement results reported in [20].

III.1 Simulation of a wide-band dynamic frequency selective mobile radio channel

The above-outlined simulation model provides separate time-domain ($H(t,f_c)$) and frequency-domain ($H(t_0,f)$) realizations of $H(t,f)$.

In this subsection we obtain bidimensional realizations of the transfer function $H(t,f)$ in order to simulate a wide-band (frequency-selective) dynamic channel. The simulation of a given environment (delay spectrum, Doppler spectrum, possible determimistic component with relative power ρ) is performed by forcing, at a given frequency (for example f_c), one of the frequency-domain realizations $H(t_0,f)$ to assume the same value of one of the time-domain realizations $H(t,f_c)$ at $t=t_0$ (that is, at the beginning of the simulation process). This forcing is repeated in the following time instants. Moreover, it is actually performed only on the phase values of the spectrum $|T_m|^2$ characterizing the chosen environment. In particular, the procedure selects that phase set of $|T_m|^2$ that makes the real and imaginary parts of $H(t_0,f)$ assume the desired values.

From a theoretical point of view, it is rather complex to establish a complete set of phase conditions to ensure the existence of such a realization (however, the possible existence of multiple solutions is not a problem). Nevertheless, it has been proved that by imposing

$$\langle |H(t_0,f)|^2 \rangle_{f\epsilon f_s} = \langle |H(t,f_c)|^2 \rangle_{t\epsilon t_s} \qquad (4)$$

the wanted realization $H(t_0,f)$ can be found after a few iterations.

To obtain the following realizations at the time instants $t>t_0$, a fewer number of iterations is necessary to get the required convergence.

Fig. 10 shows an example of bidimensional simulation as far as the envelope of the transfer function is concerned. The environment is assumed to be the CEPT/GSM typical urban ($\rho=-\infty$), with the delay profile of Fig. 1 and a mobile speed of 50 km/h. The whole simulation of Fig. 10 covers a bandwidth of about 8 MHz and lasts about 100 ms. The plot is relevant to an interesting segment lasting 5 ms and limited to a 300 kHz bandwidth (centered around f_c); the time resolution is $5\cdot10^{-4}$ s.

IV. CEPT/GSM SYSTEM CHARACTERISTICS

IV.1 Signal format and transceiver

In this paper we are concerned with the CEPT/GSM traffic channel carrying the encoded voice signal. This is transmitted by using the so-called Normal-Burst (NB) of the narrowband Time Division Multiple Access (TDMA) transmission scheme [3], [21].

Each burst (Fig. 11) contains 148 bits, including two message parts of 57 bits (plus one header bit) and a 26-bit sequence placed in between. This "midamble" allows symbol timing, carrier phase recovery, and channel estimation as outlined in the following subsection. At the two ends of each burst 3 tail bits provide a defined modulated signal immediately after ramp-up and immediately before ramp-down, and allow the channel memory due to dispersion to be exploited for the last bits as well. The guard time between two contiguous bursts is of 8.25 bits.

Eight "half" bursts are used to carry one codeword of the information signal. In fact, the voice encoder provides a block of 260 information bits every 20 ms, which are subdivided into two classes, differently encoded according to their importance for the speech quality. Class 1 includes the most important 182 bits and is split into two classes: 50 bits for "class 1a" and 132 bits for "class 1b". Class 1a bits are coded by a systematic cyclic code that adds three parity check bits, in order to detect transmission errors in the received stream. The 53 coded class 1a bits and the 132 uncoded class 1b bits plus 4 tail bits are convolutionally encoded (rate=1/2, constraint length=5) for transmission error protection. The so-obtained 378 bits together with the uncoded 78 bits of "class 2" are reordered and partitioned into 8 sub-blocks of 57 bits, which are transmitted by 8 "half" bursts according to [22].

The general block diagram of the simulated system is depicted in Fig. 12. The modulation format adopted by CEPT/GSM [23] corresponds to the Gaussian Minimum Shift Keying (GMSK) [6], with coherent demodulation, BT=0.3 and modulating data rate of 270.8 kbit/s.

Before entering the GMSK modulator, each data value $a_k\epsilon\{0,1\}$ is precoded as $a_k=a_k+a_{k-1}$. In this way, after the coherent demodulator the sampled data value on each branch is uncorrelated with respect to the preceding data values, and so the mo-demodulation process becomes practically equivalent to that of an Offset-4PSK, provided that BT is >0.25 and a sign inversion is applied to one every two samples.

The receiver includes a down-conversion and an IF RX filter (ideally equalized 7-pole Butterworth, with 3-dB bandwidth equal to $1.56f_{bit}$) and a BB RX filter (ideally equalized 5-pole Butterworth, with 3-dB bandwidth equal to $0.5f_{bit}$).

The other blocks of the receiver of Fig. 12 are discussed in the following sections.

IV.2 Synchronization and channel impulse response estimation

To recover the necessary symbol timing and carrier phase of the coherent GSM receiver, the correlation properties of suitably designed [11] binary sequences are exploited.

In particular, eight different synchronization sequences ("midambles") have been defined [21], with good cross-correlation properties in order to reduce the effects of interference among transmitters operating at the same frequency. In particular, the sequence used in this work is 00100101110000100010010111; notice that only the central 16 bits have been selected for suitable correlation properties, while the

first and last 5 bits have been added to account for the time dispersion of the channel impulse response and the time-jitter of the received signal burst.

The synchronization strategy adopted in this paper first oversamples (e.g., 4 samples/symbol) the received 26-bit midamble sequence (this is performed by the sampling processor of Fig. 12). Such an oversampling produces K (e.g., K=4 in the case of 4 samples/symbol) received midamble sequences $r_i(t)$, i=1,...,K.

Second, K complex correlation functions $R_i(t)$, i=1,...,K between the corresponding sequences $r_i(t)$ and the midamble reference complex sequence are computed. The reference complex midamble v(t) stored in the receiver (ROM of Fig. 12) is obtained by sampling the 16 central symbols of a 26-symbol MSK-modulated signal; the modulating sequence is formed by the precoded symbols $\{b_k\}$ of Fig. 12. Of course the in-phase and quadrature components of the so-obtained reference complex midamble are offset by a bit period T.

The K magnitudes $A_i(t)$, i=1,...,K of the correlation functions $R_i(t)$ are then given by

$$A_i(t) = \sqrt{[R_i^I(t)]^2 + [R_i^Q(t)]^2} \qquad (5)$$

where $R_i^I(t)$ and $R_i^Q(t)$ are the in-phase and quadrature components of $R_i(t)$, respectively.

Third the sampling instant t_0 is obtained as the peak instant of that $A_i(t)$ with maximum peak value, with a further time shift of (j-1)T/K, which takes account of oversampling; j is the value of index i corresponding to that $A_i(t)$ with maximum peak value.

Fourth, the carrier phase reference ϕ_0 is identified as

$$\phi_0 = \text{arctg}\ \frac{R_j^Q(t_0)}{R_j^I(t_0)} \qquad (6)$$

The computation of the channel impulse response h(t) necessary to the Viterbi adaptive equalizer (see subsection IV.3) is performed by using the complex correlation $R_{xv}(t)$ between v(t) and the 26 samples of the received and synchronized midamble x(t). As shown in [11], it is $R_{xv}(t)=R_{vv}(t)*h(t)$, with the autocorrelation function $R_{vv}(t)$ of v(t) equivalent to a delta function within the neighborhood of ±4 bits around its central value.

As discussed in Subsection IV.1, the demodulation process is practically equivalent to that of an Offset-4PSK.

In the case of a 16-state Viterbi adaptive equalizer, as the one used in this paper, only five consecutive samples of h(t), alternately real and imaginary, namely

$$h(t)=\sum_{i=-2}^{2} h_{-2i}^I(t_0-2it)\cdot\delta(t-2it) + j\sum_{i=-2}^{1} h_{-2i+1}^Q(t_0-(2i+1)T)\cdot\delta(t-(2i+1)T) \qquad (7)$$

have to be considered and passed to the equalizer. To do this, an "energy window" of five symbol periods is slid along h(t) to search for the sequence of five samples with maximum energy, defined as the maximum of

$$E_j = \sum_{i=-4+j}^{j} \{[h^I(t_0-iT)]^2+[h^Q(t_0-iT)]^2\},\ j=0,...,4 \qquad (8)$$

IV.3 Viterbi adaptive equalizer

This kind of equalizer does not, in the strict sense, attempt to equalize the channel impulse response. Rather, it uses the knowledge of the channel impulse response (through an estimation technique) and of the received signal in order to find the most likely transmitted data sequence. Its performance is therefore dependent on the available estimate of the channel impulse response as well as on the sample timing and carrier phase recovery, as discussed in the previous subsection.

It is well known that in a maximum likelihood sequence estimation [6], [24], a metric is required to discriminate among all the possible transmitted sequences: the most likely sequence is that which maximizes tha likelihood function [6], [24].

In general, computation of the likelihood function requires passing the received signal through a matched filter with impulse response h*(-t) followed by a processing of the sampled outputs of the matched filter. A brute force approach of computing the value of the likelihood function for each of the possible data sequences would be very inefficient. Instead, the Viterbi algorithm reduces the computational burden by observing that the incremental metric at time instant k=n depends only on the sequence

$$\alpha_n^m,\ \alpha_{n-1}^m,...,\alpha_{n-L}^m\ ,$$

where α_k are, in the case of the CEPT/GSM radio signal, alternately real and imaginary, L is the number of significant interfering samples of h(t), m denotes the generic mth sequence.

This means that we have to deal only with the last L+1 bits of the sequence concerned. Moreover, the Viterbi algorithm can discard all but the most likely sequence, called "survivor", at k=n. Each survivor is associated with a state which is characterized by a set of L values $\alpha_n,\ \alpha_{n-1},...,\alpha_{n-L+1}$, since these are the only values required for computation of the next incremental metric for the subsequent extensions of this sequence.

To summarise, at each instant k all sequences joining the same state have their metrics compared and a survivor is chosen. The process is repeated for each of the 2^L states. For binary signalling each survivor gives rise to two extended sequences, but at instant k+1 these are pruned back to their original number by metric comparison of the two incoming sequences to each state.

Further simplifications to the incremental metric computation can still be made for GMSK by observing that $\alpha_k=\pm1$ or $\pm j$ and by noting that at k=n either the real or the imaginary part of the signal y_n of Fig. 12 is needed, but not both. Hence, the matched filter implementation can be somewhat simplified. Finally, a term of the incremental metric can only have 2^{L+2} possible values, and hence these can be stored in a look-up table prior to the Viterbi algorithm operation, to be recalled when required. In practice, in this paper we have computed the incremental metric Λ_{mn} through the following formula

$$\Lambda_{mn} = \Lambda_{m(n-1)} + \text{Re}\{(\alpha_n^m)^*(y_n-P_s)\} \qquad (9)$$

where P_s is a complex number read from a look-up table corresponding to the state s for which a survivor is being searched.

To perform the demodulation of the received signal burst, the Viterbi adaptive equalizer starts its operation from the information bits close to the midamble, which should undergo similar channel distortions, and works rightward and leftward (the received time slot is completely stored before starting its processing).

The Viterbi equalizer described above is derived from the idea first proposed in [25], and was adopted in [10], [11]. It requires only four additions per state and does not require any noise whitening because operates on the sampled outputs of the matched filter.

In this paper we have further simplified the equalizer scheme by using a fixed filter rather than a matched filter, always without noise whitening (Fig. 12). Since such a filter is the bandpass filter already existent in the receiver described in Subsection IV.1, essentially no processing is required apart from signal sampling before the Viterbi algorithm. This kind of receiver can be considered to be matched to the average channel and degradation due to noise enhancement will appear if the channel transfer function shows notches near the carrier frequency. On the other hand, the absence of a matched filter will increase the sensitivity of the receiver to initial timing errors. Results on these topics will be presented in future papers.

IV.4 System simulation

The Viterbi equalizer described above is initialized through a channel impulse response estimation, together with sample timing and carrier phase recovery, during the midamble transmission period at the center of the basic time slot of Fig. 11. Then no tracking of the changes in the channel response over the two information data transmission periods is performed. Such changes in the channel response are simulated through the propagation characteristic modelling technique of Sections II and III, which provides a set of Time and Frequency-dependent Linear Filters (TFLFs) $\{H_i(t,f)\}_{i=1}^{M}$.

Of course the number of $H_i(t,f)$ affecting a given time slot depends on the vehicle speed v. For example, when v≅50km/h eleven different H(t,f) have to be considered per each time slot. This means that each $H_i(t,f)$ "covers" 156.25/11≅14.2 bits, during which the channel transfer function is meant to be constant.

Consequently, the Viterbi equalizer is initialized according to the channel characteristics corresponding to the central filters $H_i(t,f)$, but it will have to equalize the channel distortions corresponding to the preceding $H_i(t,f)$ (leftward operation) and to the following $H_i(t,f)$ (rightward operation). The same operation is repeated in the following time slots, by considering different sets of eleven $H_i(t,f)$. The higher the vehicle speed, the greater the equalizer mismatching.

Moreover, since the signal bursts are transmitted within a TDMA frame with 8 time slots, as specified in [22], the sets of consecutive filters $H_i(t,f)$ are drawn from $\{H_i(t,f)\}_{i=1}^{M}$ with the same time periodicity.

Our simulation program, which is frequency-domain based, builds the distorted bit sequence of the basic time slot by performing eleven (in the case of v=50km/h) filterings of the modulated signal through eleven $H_i(t,f)$ and by joining the pertaining 14.2 bits in the right order. This operation has to be repeated for a number of times large enough to get the required statistical completeness.

Preliminary BER results of the above described Viterbi equalizer are given in Fig. 13 for v=50 km/h. In particular, the BER curves for the distorted channels are relevant to the uncoded class 2 bits, and to the coded bits of classes 1a and 1b. In the latter case an ideal soft-decision technique has been adopted.

ACKNOWLEDGEMENTS

The authors wish to thank Mr. E. Ercolin for his help in performing the computer simulations.

REFERENCES

[1] "Status of studies, experiments and harmonization process in Europe", Session 1 in Proc. Int. Conf. on Digital Land Mobile Radio Communications, Venice, Italy, June 30-July 3, 1987

[2] Sessions 3÷6, Proc. Third Nordic Seminar on Digital Land Mobile Radio Communication, Copenhagen, Denmark, Sept. 13-15, 1988

[3] CEPT/GSM Rec. 05.05

[4] E. Damosso, "Wide-band propagation measurements at 900 MHz", Alta Frequenza, Vol. LVII, No. 2, pp. 65-74, Feb.-March 1988

[5] T. Aulin, "A modified model for the fading signal at a mobile radio channel", IEEE Trans. Vehic. Tech., Vol. VT-35, No. 3, pp. 182-203, 1979

[6] J.G. Proakis, Digital Communications. New York, N.Y.: Mc Graw-Hill, 1983

[7] G. D'Aria, R. Piermarini, and V. Zingarelli, "Fast adaptive equalizers for narrowband TDMA mobile radio", submitted to IEEE Trans. Vehic. Tech., 1989

[8] G. D'Aria and V. Zingarelli, "Adaptive baseband equalizers for narrowband TDMA/FDMA mobile radio systems", Proc. Int. Conf. on Digital Land Mobile Radio Communications, Venice, Italy, pp. 280-289, June 30-July 3, 1987

[9] "Adaptive Equalization: Performance Summary", COST 207 WG3, Doc. TD(87)53

[10] G. D'Aria and V. Zingarelli, "Results on Fast-Kalman and Viterbi adaptive equalizers for mobile radio with CEPT/GSM system characteristics", IEEE Globecom '88, Hollywood, FL, Nov. 28-Dec. 1, 1988

[11] G. D'Aria and V. Zingarelli, "Design and performance of synchronization techniques and Viterbi adaptive equalizers for narrowband TDMA mobile radio", Proc. Third Nordic Seminar on Digital Land Mobile Radio Communication, Copenhagen, Denmark, Sept. 13-15, 1988

[12] R.H. Clarke, "A statistical theory of mobile-radio reception", BSTJ, vol. 47, pp. 957-1000, July-August 1968

[13] W.C. Jakes Jr., Microwave mobile communication, New York, NY: Wiley & Sons, 1974

[14] W.C.Y. Lee, Mobile communication engineering. New York, NY: McGraw-Hill, 1982

[15] "Effects of the urban structure on land mobile propagation at 900 MHz", COST 207 Doc. TD(86)23, Paris, Sept. 1986

[16] Y. Okumura, E. Ohmori, T. Kawano, and K. Fukuda, "Field strength and its variability in VHF and UHF land-mobile radio service", Rev. Elec. Comm. Lab., vol. 16, No. 9-10, pp. 825-873, 1968

[17] M.F. Ibrahim and J.D. Parsons, "Signal strength prediction in built-up areas; Part 1: Median signal strength", IEE Proc. Part F, vol. 130, No. 5, pp. 377-384, 1983

[18] J.F. Ossanna, Jr., "A model for mobile radio fading due to building reflections: theoretical and experimental fading waveform power spectra", BSTJ, No. 11, pp. 2935-2971, 1964

[19] S.O. Rice, "Statistical properties of a sine wave plus random noise", BSTJ, vol. 27, No. 1, pp. 109-157, 1948

[20] P. Melancon and J. Le Bel, "A characterization of the frequency selective fading of the mobile radio channel", IEEE Trans. Vehic. Tech., vol. VT-35, No. 4, pp. 153-161, Nov. 1986

[21] CEPT/GSM Rec. 05.02

[22] CEPT/GSM Rec. 05.03

[23] CEPT/GSM Rec. 05.04

[24] S. Benedetto, E. Biglieri, and V. Castellani, Digital Transmission Theory. Englewood Cliffs, NJ: Prentice Hall, 1987

[25] G. Ungerboeck, "Adaptive maximum likelihood receiver for carrier modulated data transmission systems", IEEE Trans. Commun., vol. COM-22, No. 5, pp. 624-636, May 1974

[26] F. Muratore and V. Palestini, "A computer simulation program for TDMA systems", Proc. Int. Conf. on Digital Land Mobile Radio Communications, Venice, Italy, pp.290-299, June 30-July 3, 1987

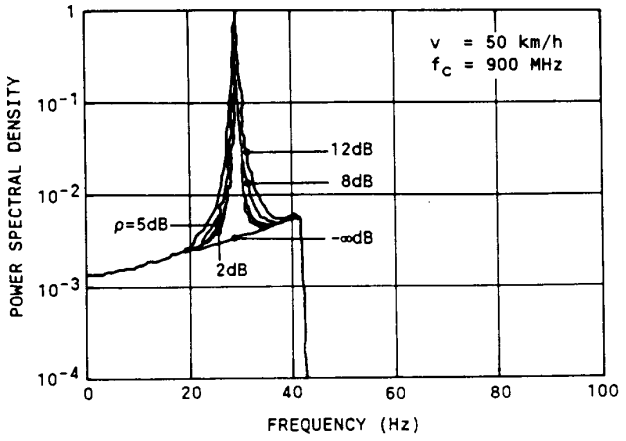

Fig. 1 - Average simulated spectra of $Re\{H(t,f_c)\}$ (or $Im\{H(t,f_c)\}$)

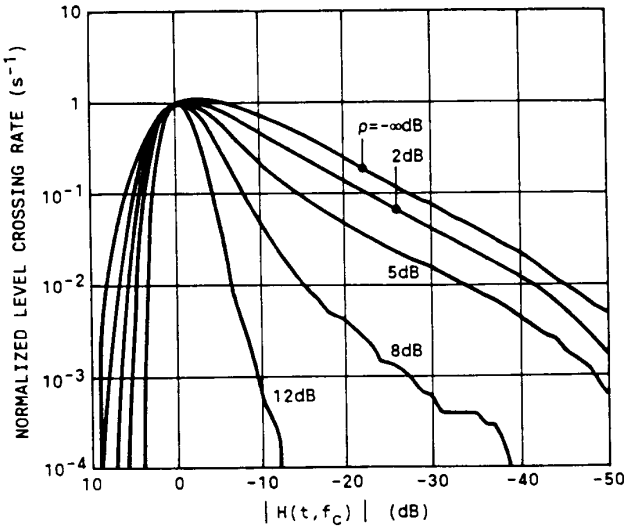

Fig. 2 - Normalized level crossing rate of $|H(t,f_c)|$

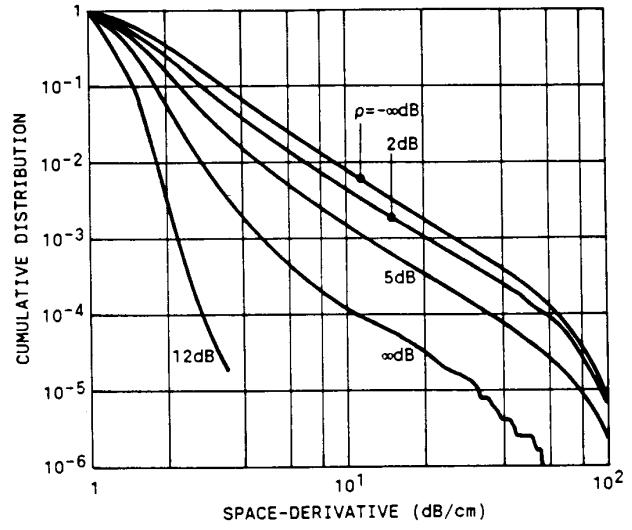

Fig. 3 - Space-derivative statistics of $|H(t,f_c)|$

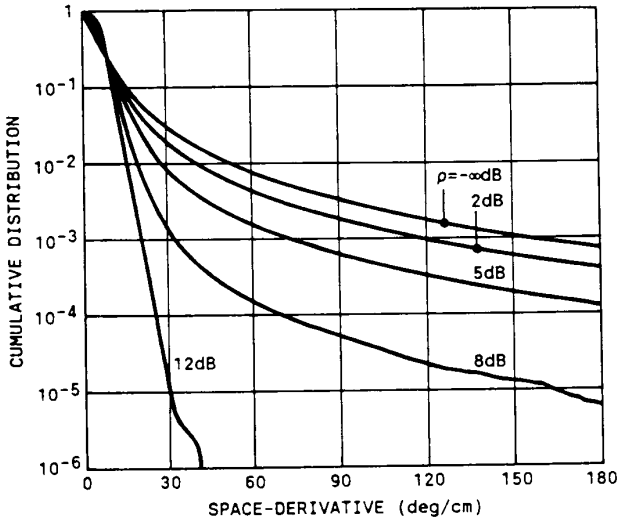

Fig. 4 - Space-derivative statistics of $\phi_H(t,f_c)$

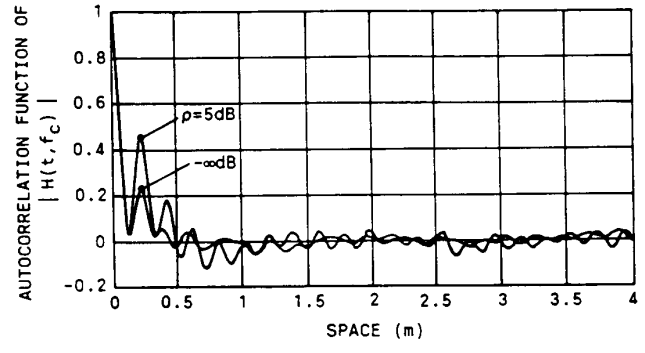

Fig. 5 - Space-autocorrelation function of $|H(t,f_c)|$

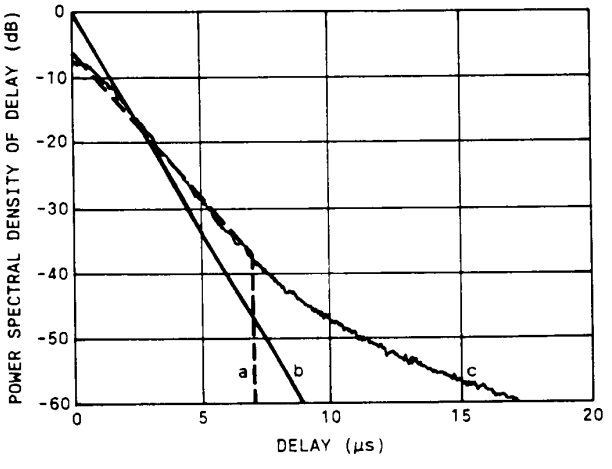

Fig. 6 - Delay profiles of modulus and real (or imaginary) part of $H(t_0,f)$

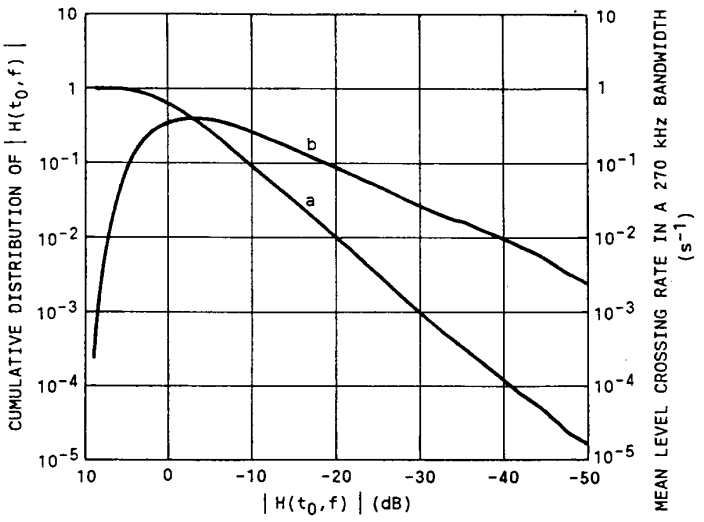

Fig. 7 - Instantaneous channel statistics:
a) Cumulative distribution of $|H(t_0,f)|$
b) Mean level crossing rate in a 270 kHz bandwidth

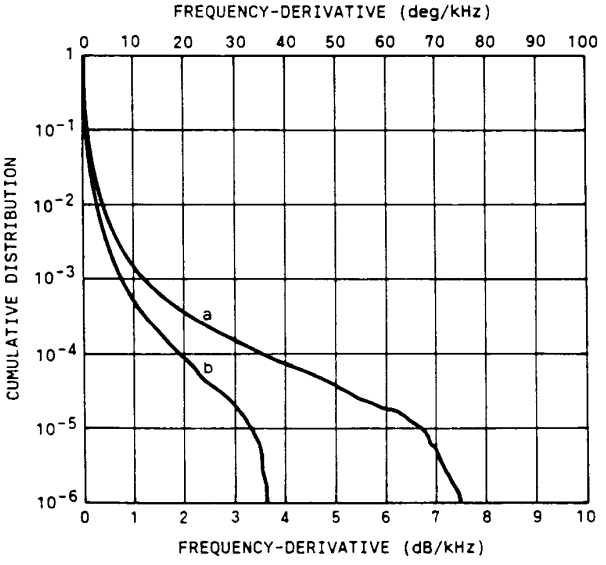

Fig. 8 - Frequency-derivative statistics of the instantaneous channel:
a) Cumulative distribution of $|H(t_0,f)|$ derivative
b) Cumulative distribution of $\phi_H(t_0,f)$ derivative

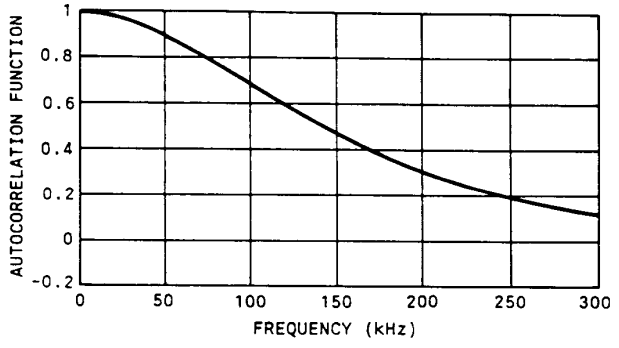

Fig. 9 - Frequency-autocorrelation function of $|H(t_0,f)|$

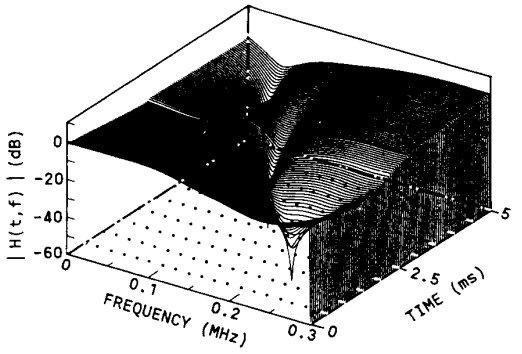

Fig. 10 - Example of simulation of $|H(t,f)|$

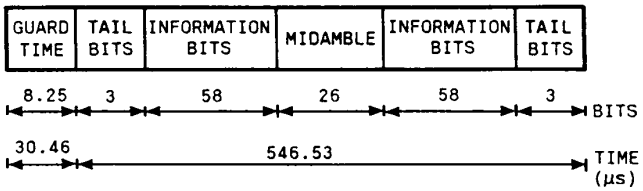

Fig. 11 - Basic time slot structure

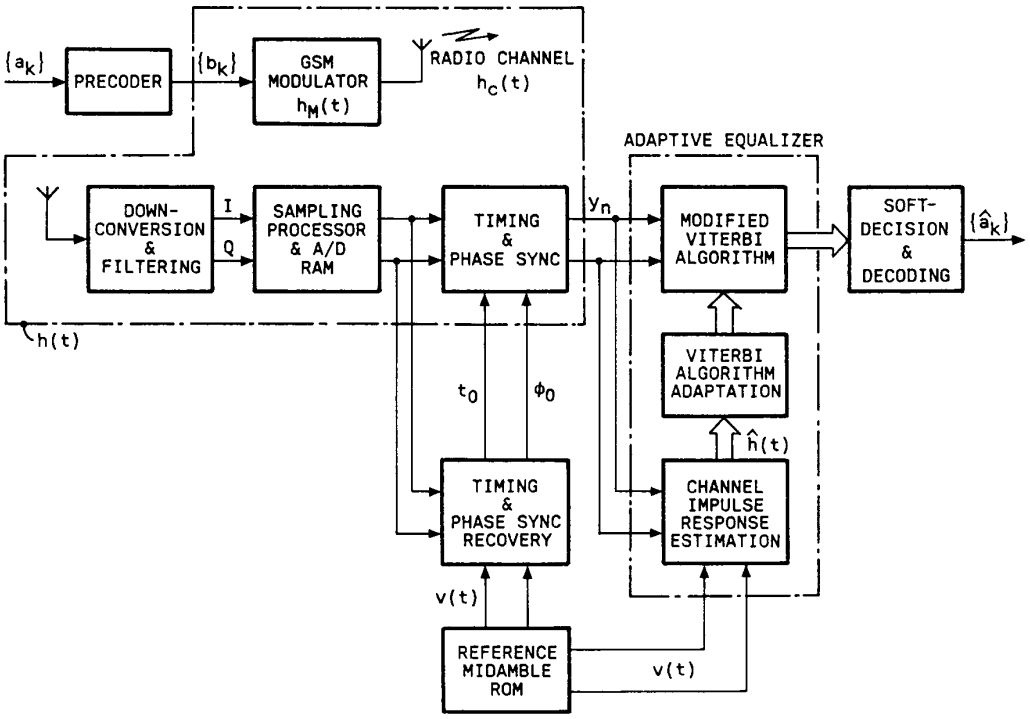

Fig. 12 - Block diagram of the simulated CEPT/GSM system

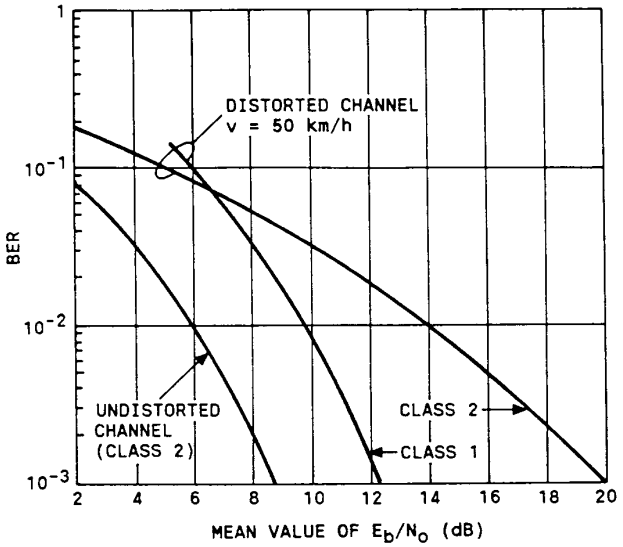

Fig. 13 - Bit error rate of the CEPT/GSM system with a 16-state Viterbi equalizer, in the case of typical urban propagation model